Available online at www.sciencedirect.com

ScienceDirect

Energy Procedia 38 (2013) 147 – 152

Energy Procedia

SiliconPV: March 25-27, 2013, Hamelin, Germany

Predicting solar cell efficiencies from bulk lifetime images of multicrystalline silicon bricks

Bernhard Mitchell[a]*, Hannes Wagner[a,b], Pietro P. Altermatt[b], Thorsten Trupke[a,c]

[a]*Australian Centre for Advanced Photovoltaics, School of Photovoltaic and Renewable Energy Engineering, University of New South Wales, Sydney, NSW 2052, Australia*

[b]*Leibniz University of Hanover, Department Solar Energy, Appelstr. 2, 30167 Hannover, Germany*

[c]*BT Imaging, 1 Blackburn St, Surry Hills, NSW 2010, Australia*

Abstract

We present a model for predicting the solar cell efficiency potential of multicrystalline silicon bricks prior to sawing. Three model inputs are required: bulk lifetime images from the side faces of the bricks, the cell manufacturing process, and its gettering action. The model is set up with numerical device and circuit simulations, but may afterwards be parameterized for inline application. In the example shown here, we chose literature data to quantify the increase in bulk lifetime caused by phosphorus gettering of impurities during cell manufacturing. Our proposed model enables manufacturers to (i) assess initial brick quality in relation to their specific cell production line, (ii) to exclude certain parts of the bricks from cell manufacturing, and (iii) to adjust cell manufacturing to initial material quality. The specific gettering efficiency and cell process can be fed into the model dynamically and need to be calibrated ideally for each material manufacturer and each cell production line. The model presented here can be extended to cast mono and dendritically grown bricks.

Keywords: Lifetime; Bricks; Multicrystalline; Efficiency; Device modeling; Spice circuit modeling

1. Introduction

There have been efforts [1–3] to predict solar cell efficiencies prior to manufacturing, based on lifetime measurement of multicrystalline or mono-like as-cut wafers or silicon bricks often linked to

* Corresponding author. Tel.: +61-433-267540
E-mail address: bernhard.mitchell@unsw.edu.au

doi:10.1016/j.egypro.2013.07.261

impurity concentrations. This is not surprising, because such predictions enable manufactures to exclude unsuitable wafers from cell production and hence to save costs.

Lifetimes are a suitable parameter as they strongly influence cell efficiency. However, it is well known that lifetimes change during processing due to gettering, contamination and hydrogenation. Thus, it is an intricate task to use measured initial lifetimes for predicting cell efficiency. In as-cut wafers, bulk lifetimes are largely inaccessible, because surface recombination limits the measured lifetime [4]. However, in silicon bricks, bulk lifetimes can be measured, as was demonstrated in [5–9]. This can be exploited for efficiency predictions.

It was recently shown [10] that device modeling is capable of reproducing experimentally achieved mc-Si cell efficiency when lifetime images are used as model input. For example, the emitter and BSF of fabricated cells were etched off, the new surfaces were passivated at low-temperature, and a lifetime image was taken. When feeding these lifetimes into the device model, V_{oc} was reproduced within three mV.

In this paper, we combine photoluminescence detected bulk lifetimes and device modeling to predict solar cell efficiencies as a function of brick height. We incorporate published gettering data and thus demonstrate the principle of this promising approach.

2. Bulk lifetime measurements

The bulk excess carrier lifetimes beneath the side faces of silicon bricks, $\tau_b(x,y)$, can be measured with high spatial resolution by photoluminescence spectral intensity-ratio (PLIR) imaging. The variable x represents the lateral coordinate and y the brick height, which is the growth direction of the crystal. Fig. 1 shows the PLIR detected $\tau_b(x,y)$ image of a typical brick side face. We use an improved imaging procedure [6] for gaining data throughout the whole brick height, and we obtain data with reasonable confidence even in the high-impurity zones at the bottom and the top of the brick, where lifetimes drop below 5 µs. The bulk lifetimes range from 150 µs in the centre to ~ 0.5 µs at the bottom and the top.

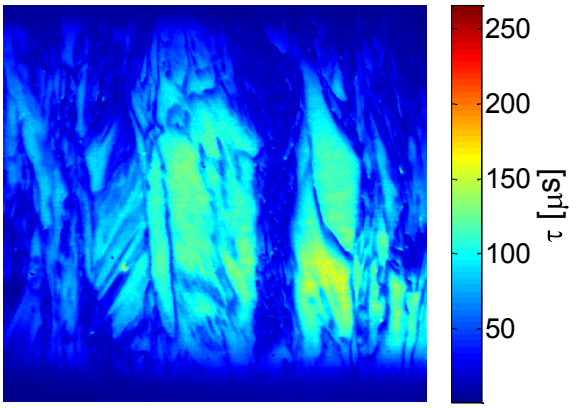

Fig. 1: Bulk lifetime image as measured at a brick face using the PLIR technique [5].

3. Process induced changes to lifetime

Carnel et al. [11] and Tan et al. [12] compared lifetimes in wafers before and after gettering. We extract the bulk lifetime before and after gettering from Carnel et al. [11] as shown in Fig. 2(a). The ratio

between both curves was applied to the PLIR detected $\tau_b(x,y)$ image shown in Fig.1 to obtain the gettered bulk lifetime $\tau_b(x,y)$ illustrated in Fig. 2(b).

The gettering data and the PLIR detected bulk lifetime contains significant error in the very top and bottom section of the brick (areas indicated in Fig. 2(a) with dashed line). We therefore do not investigate these areas quantitatively and only show cropped brick images. We note that this does not affect the analysis, since these areas will not be utilized for solar cell manufacturing in any case.

We note that the ratio in the very top and bottom section of the brick was measured with extremely high values and likely contains significant errors. We indicate this area with a dashed line in Fig. 2(a). Future experiments need to reinvestigate the gettering efficacy in this region.

It is important to include the gettering-induced changes to lifetime in our model, because Carnel et al. [11] and Schueler et al. [13] have shown that a consistent correlation between brick quality and cell efficiency can only be found in relation to the gettered – not the initial – bulk lifetime. Effective phosphorus and temperature assisted gettering during cell manufacturing removes most of the lifetime limiting impurities such as iron, or clusters them into less recombination active states, which is referred to as internal gettering [5,6].

In order to fine-tune our model to a specific manufacturer, an experimental assessment of the gettering efficiency needs to be done initially. One method is comparing neighbouring wafers at various positions within the brick, where every second wafer is processed into a solar cell and then etched back for a final bulk lifetime measurement. Such an experimental calibration would have the advantage that also improvements in $\tau_b(x,y)$ due to hydrogenation, aluminium gettering and changes in dislocations densities [16] would be included. In our present example, we only include phosphorus gettering.

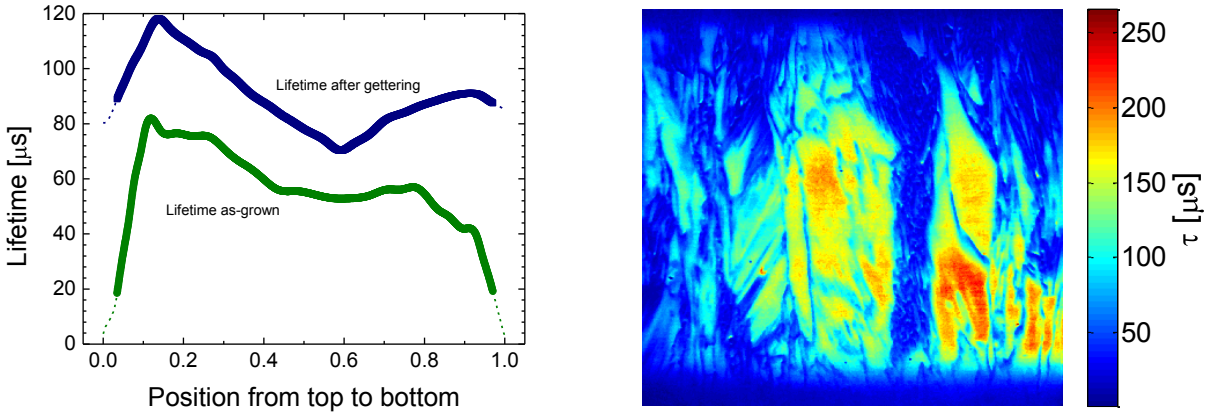

(a) (b)

Fig. 2: (a) Brick lifetime before and after gettering as measured by Carnel et al. [11]. The ratio between both curves was used to recalculate the lifetime image in Fig. 1. The data on the very bottom and top section of the brick is expected to carry a larger error. It is therefore drawn in a dashed line. (b) Bulk lifetime after phosphorous gettering, calculated from Fig. 1 using (a).

4. Device simulations

In order to quantify the brick's cell efficiency potential, we proceed in two steps. Firstly, we simulate mc-Si solar cells with the following approach. The $\tau_b(x,y)$ values at any height y of the brick is discretized in a lifetime histogram having a number n of lifetime values $\tau_{sim,i}$ with corresponding frequencies A_i. We then simulate, using Sentaurus Device [13], a sequence of n monocrystalline Si cells in two dimensions,

each having a homogeneous lifetime $\tau_{sim,i}$, and obtain their I-V curves $I(V)_{mono,i}$. To calculate the I-V curve of the mc-Si cell, $I(V)_{multi}$, these simulated $I(V)_{mono,i}$ curves are fed to a SPICE circuit model, using the frequencies A_i as area factors. The circuit then approximates the lateral current flow within both the semiconductor material and the front metal fingers. Finally, the resulting $I(V)_{multi}$ curve provides the efficiency η.

In a second step, we correlate the measured lifetime values with mc-Si cell efficiencies with the following approach. Fig. 3 shows the efficiency η resulting from the $I(V)_{mono,i}$ curves for two different cell designs: a standard design and a cell with improved emitter, rear back surface field and optimized grid spacing. As η depends on the manufacturing process [17], we call Fig. 3 a cell process curve (CPC). With the CPC, each lifetime value in the brick can be translated to a corresponding efficiency value, so the whole lifetime image can be translated into an efficiency images. In short, a cell manufacturer needs to simulate a CPC of a production line only once, and then this CPC alone can be used to predict cell efficiency from the PLIR detected $\tau_b(x,y)$ image and the established gettering ratio.

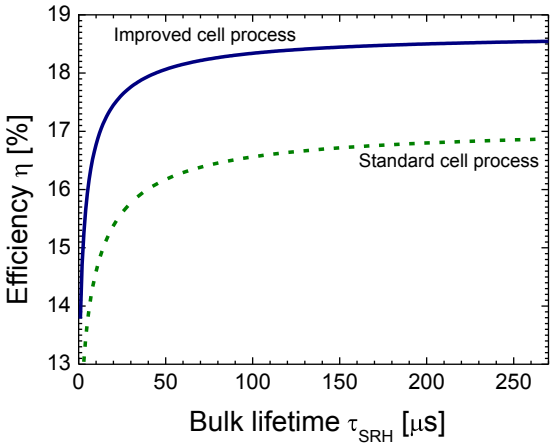

Fig. 3: Cell efficiency as a function of homogeneous bulk lifetime, obtained from numerical device simulations. A standard and an improved cell manufacturing process are shown.

5. Results

The brick is now analyzed with the above described methods. Each lifetime value from Fig.2(b) is translated with the CPC (of the improved cell process in Fig. 3) to the corresponding cell efficiency and is depicted in Fig. 4(a). In Fig. 4(b), mc-Si cell efficiencies are shown in dependence of the position within the brick. Note that the efficiencies in Fig. 4(b) are not obtained by a simple mathematical averaging procedure of Fig. 4(a), but from combined device and a circuit simulation as described in part one of section 4. This is a crucial step for a useful brick quality assessment. Otherwise, the correlation between initial brick lifetime and final cell efficiency becomes too vague.

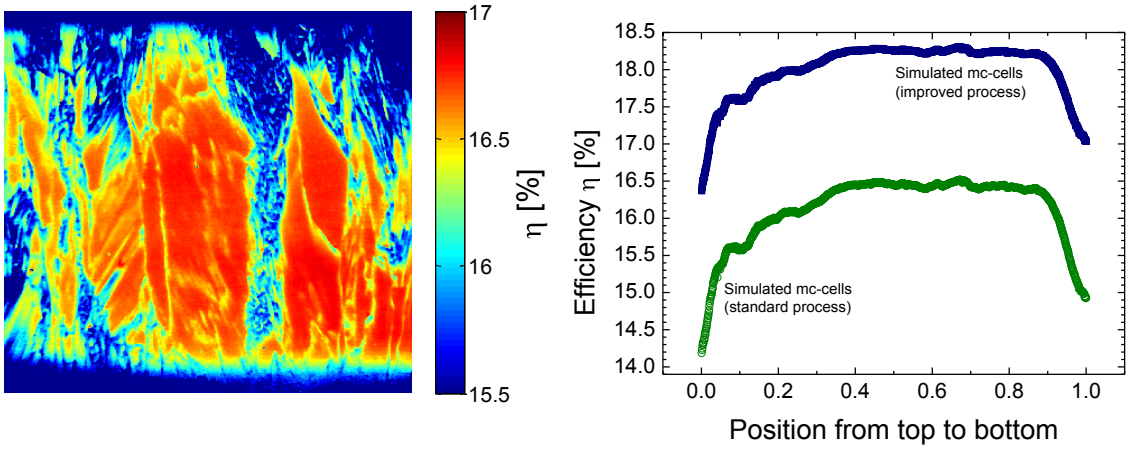

Fig. 4: (a) Efficiency image, obtained from recalculating Fig. 2(b) with the simulated curve in Fig. 3; (b) Simulated mc-cell efficiency shown in dependence of the position within the brick in Fig. 4(a). Shown are the results for two different cell processes (see Fig. 3).

6. Conclusion and outlook

A method of predicting mc-Si cell efficiency from lifetime measurements of mc-Si bricks has been demonstrated in principle. The method uses a combination of (i) photoluminescence detected bulk lifetime images of brick faces, (ii) a gettering ratio to quantify the changes in lifetimes due to cell manufacturing, and (iii) numerical device simulation. Tasks (ii) and (iii) need be done only once for a certain cell manufacturing process, yielding the gettering ratio and the cell process curve (CPC). Then, many incoming bricks may be quickly assessed by task (i) using the simple curves that resulted from tasks (ii) and (iii). We expect that, with this method, suitable parts of the bricks can be selected more precisely and in a strongly simplified way.

In this paper, only literature data for gettering ratios are used. In practical applications, the influence of gettering on lifetimes needs to be assessed because this data is always specific to each material manufacturer and to each cell manufacturing process. Also, each production line will need to be modeled individually. A more general approach might be possible if impurity concentrations are already known on brick level [2,18].

Finally, it will need to be investigated in more detail how accurate cell efficiencies can be predicted of wafers that are effectively only measured on their side faces.

Acknowledgements

This research has been supported by the Australian Government through the Australian Renewable Energy Agency (ARENA)

References

[1] R.A. Sinton, Predicting multi-crystalline solar cell efficiency from life-time measured during cell fabrication, in: 3rd World Conference on Photovoltaic Energy Conversion, Osaka, 2003: pp. 1028–1031.

[2] R.A. Sinton, T. Mankad, S. Bowden, N. Enjalbert, Evaluating silicon blocks and ingots with quasi-steady-state lifetime measurements, in: Proceedings of the 19th European Photovoltaic Solar Energy Conference, Paris, France, 2004: pp. 520–523.

[3] J. Hofstetter, D.P. Fenning, M.I. Bertoni, J.F. Lelièvre, C. del Cañizo, T. Buonassisi, Impurity-• to-• efficiency simulator: predictive simulation of silicon solar cell performance based on iron content and distribution, Progress in Photovoltaics: Research and Applications. 19 (2011) 487–497.

[4] K. Bothe, R. Krain, R. Falster, R. Sinton, Determination of the bulk lifetime of bare multicrystalline silicon wafers, Progress in Photovoltaics: Research and Applications. 18 (2010) 204–208.

[5] B. Mitchell, T. Trupke, J.W. Weber, J. Nyhus, Bulk minority carrier lifetimes and doping of silicon bricks from photoluminescence intensity ratios, Journal of Applied Physics. 109 (2011) 083111.

[6] B. Mitchell, J.W. Weber, D. Walter, D. Macdonald, T. Trupke, On the method of photoluminescence spectral intensity ratio imaging of silicon bricks : advances and limitations, Journal of Applied Physics. 112 (2012) 063116.

[7] B. Mitchell, J. Greulich, T. Trupke, Quantifying the effect of minority carrier diffusion and free carrier absorption on photoluminescence bulk lifetime imaging of silicon bricks, Solar Energy Materials and Solar Cells. 107 (2012) 75–80.

[8] S. Johnston, F. Yan, M. Al-Jassim, Quality Characterization of Silicon Bricks using Photoluminescence Imaging and Photoconductive Decay, 38th IEEE Photovoltaic Specialists Conference. (2012) 2–6.

[9] J.S. Swirhun, R.A. Sinton, M.K. Forsyth, T. Mankad, Contactless measurement of minority carrier lifetime in silicon ingots and bricks, Progress in Photovoltaics: Research and Applications. 19 (2011) 313–319.

[10] H. Wagner, M. Müller, G. Fischer, P.P. Altermatt, Modelling of Multicrystalline Si Solar Cells Based on Lifetime Distributions, in: Proceedings of the 27th Photovoltaic and Solar Energy Conference, Frankfurt, Germany, 2012.

[11] L. Carnel, J. Nyhus, K. Helland, Influence of wafer quality on cell performance, Photovoltaics International 7th Edition. (2010) 45–48.

[12] J. Tan, D. Macdonald, N. Bennett, D. Kong, a. Cuevas, I. Romijn, Dissolution of metal precipitates in multicrystalline silicon during annealing and the protective effect of phosphorus emitters, Applied Physics Letters. 91 (2007) 043505.

[13] N. Schüler, D. Mittelstrass, K. Dornich, J.R. Niklas, H. Neuhaus, Next Generation Inline Minority Carrier Lifetime Metrology on Multicrystalline Silicon Bricks For PV, in: Proceedings of the 35th IEEE Photovoltaic Specialist Conference, Honolulu, Hawaii, 2010.

[14] A. Liu, Y. Fan, D. Macdonald, Interstitial iron concentrations across multicrystalline silicon wafers via photoluminescence imaging, Progress in Photovoltaics: Research and Applications. 19 (2011) 649–657.

[15] J. Hofstetter, J.F. Lelièvre, C. del Cañizo, A. Luque, Study of Internal versus External Gettering of Iron during Slow Cooling Processes for Silicon Solar Cell Fabrication, Solid State Phenomena. 156-158 (2009) 387–393.

[16] H. Choi, M. Bertoni, J. Hofstetter, Dislocation Density Reduction During Impurity Gettering in Multicrystalline Silicon, IEEE Journal of Photovoltaics. 3 (2012) 189 – 198.

[17] B. Michl, M. Rüdiger, J.A. Giesecke, M. Hermle, W. Warta, M.C. Schubert, Efficiency limiting bulk recombination in multicrystalline silicon solar cells, Solar Energy Materials and Solar Cells. 98 (2012) 441–447.

[18] K. Dornich, N. Schüler, B. Berger, J.R. Niklas, Fast, high resolution, inline contactless electrical semiconductor characterization for photovoltaic applications by microwave detected photoconductivity, Materials Science and Engineering: B. (2013) (in press).